

M. MISZCZYK*, H. PAUL**, J.H. DRIVER***, CL. MAURICE***

MICROSTRUCTURE AND TEXTURE EVOLUTION DURING ANNEALING OF PLANE STRAIN COMPRESSED Al AND Al-1%Mn ALLOY SINGLE CRYSTALS

EWOLUCJA MIKROSTRUKTURY I TEKSTURY PODCZAS WYŻARZANIA MONOKRYSTAŁÓW Al I Al-1%Mn ODKSZTAŁCANYCH W PŁASKIM STANIE ODKSZTAŁCENIA

The microstructure and the texture evolutions of partly recrystallized samples of pure Al and the Al-1%wt.Mn alloy have been characterized by a high resolution SEM/EBSD. The single crystals of the Goss{110}<001> and brass{110}<112> orientations, stable in the plane strain compression, were deformed in a channel-die up to 60% to develop a homogeneous structure composed of two sets of symmetrical primary microbands and then shortly annealed. It is documented that the orientations of the initial nucleus were scattered but not accidental. The disorientation axes in the orientation relationship across the recrystallization front usually coincide with one of the <112>, <221>, <102> or <111> crystallographic directions and were rather rarely close to the <110> or <001> directions. The disorientation axis of the <111>- type is only one of the few most often observed.

Keywords: microstructure, texture, plane strain compression, nucleation & recrystallization

Przemiany tekstury w początkowych stadiach rekrytalizacji są przedmiotem intensywnych badań, zwłaszcza tych które dotyczą półwyrobów płaskich stosowanych w przemyśle do wytwarzania opakowań drogą głębokiego tłoczenia. W niniejszej pracy wykorzystano wysokorozdzielczy system SEM/EBSD do analizy tych zmian w nieswobodnie ściskanych próbkach aluminium oraz stopu Al-1%Mn. Dla przejrzystości prowadzonej analizy, w badaniach wykorzystano próbki monokrystaliczne, o orientacjach stabilnych w płaskim stanie odkształcenia, tj. Goss{110}<001> i brass{110}<112>. Poddano je nieswobodnemu ściskaniu (powszechnie uznawanemu za modelowe przybliżenie procesu walcowania) do 40% i 60%, a następnie analizowano ich zachowanie w początkowych stadiach rekrytalizacji. W stanie po deformacji obserwowano jednorodną strukturę dwu symetrycznie usytuowanych rodzin mikropasm, która w procesie rekrytalizacji sprzyjała pojawieniu się nowych ziaren. Udokumentowano, że orientacje początkowych ziaren, wyrastających ze struktury stanu zdeformowanego nie są przypadkowe, i tylko ściśle określona liczba grup orientacji może się pojawić w początkowym stadium wyżarzania. Dezorientacja obliczona poprzez migrujący front rekrytalizacji związana jest najczęściej z rotacją dookoła kierunków krystalograficznych typu <112>, <221>, <102> lub <111>, oraz rzadziej <110> lub <001>. Oś dezorientacji typu <111> jest tylko jedną z kilku częściowo spotykanych.

1. Introduction

During the primary recrystallization, the orientations of the new grains are thought to originate from the set of orientations that are present within the deformed state [1, 2]. However, the nature of this relation has been the subject of a major discussion over the last few decades. One of the main controversies concerns the lack of a well-defined selection system for the rotation axes in the misorientation relation between the nuclei and the deformed areas and, more generally, the fre-

quently observed failure of the 40° <111>-type relations [3-8].

To improve our understanding of the recrystallization texture formation in rolled sheet strips, it is useful to examine the characteristic behaviour of deformed grains. Specimens composed of single crystals with well-known initial orientation provide the best opportunities for these detailed studies. For simplicity, it is important that the crystallite orientations do not change significantly after the deformation [4, 5]. This has been done by means of applying the single crystals of the stable ori-

* POLISH ACADEMY OF SCIENCES, INSTITUTE OF METALLURGY AND MATERIALS SCIENCE, KRAKOW, POLAND

** OPOLE UNIVERSITY OF TECHNOLOGY, FACULTY OF MECHANICS, OPOLE, POLAND

*** ECOLE NATIONALE SUPERIEURE DE SAINT ETIENNE, CENTRE SMS, SAINT ETIENNE, FRANCE

orientations. For the face centred cubic metals, there are two orientations, stable in the plane strain compression (PSC) up to very high strains, i.e. $\{110\}\langle 001\rangle$ (*Goss*) and $\{110\}\langle 112\rangle$ (*brass*) [10, 11].

The aim of this study is to examine the crystallographic aspects of the recrystallization nuclei occurrence. Since the orientations of the above crystals disorient each other by a 35° rotation around ND $\parallel \langle 110\rangle$, where ND is the normal direction, this opens the possibility to investigate the influence of different slip configurations, active in deformation, on the crystallographic aspects of nucleation in annealing, by means of identifying the specific disorientation axes across the recrystallization front. In fact, the issue related to the definition of the rotation axes is the question of the mechanisms governing the thermally activated dislocation movement in annealing. The use of pure aluminium and the Al-1%wt.Mn alloy, (the materials with a high stacking fault energy in which the mechanical and recrystallization twinning are strongly limited) makes it easier to identify the mechanisms responsible for the texture transformation during the initial stages of annealing.

2. Material and methods

A high purity Al (99.998%) and the Al-1%wt.Mn alloy single crystals with initial *Goss* $\{110\}\langle 001\rangle$ and *brass* $\{110\}\langle 112\rangle$ orientations were channel-die compressed by 40% and 60% to develop a homogeneous structure composed of two sets of symmetrical primary microbands [10, 11]. The single crystals were grown by the modified Bridgman technique (horizontal solidification) with the use of split graphite moulds. The exact orientations of the samples before compression were checked by the back reflection Laue X-ray. The samples were compressed in a channel-die rig at a nominal strain rate of $\sim 10^{-4}\text{s}^{-1}$. The as-deformed samples were then slightly annealed to develop a state of partial recrystallization. For both metals, the recrystallization was observed to occur after a short annealing at temperatures ranged between 330°C and 420°C , and for the time periods between 20s and 30s. The specimens were examined with the use of a scanning electron microscopy (SEM) – JEOL JSM 6500F – equipped with a field emission gun (FEG) and the electron backscattered diffraction (EBSD) facility. The local orientations were mostly measured on the longitudinal plane, i.e. ND-ED, where ED is the extension (rolling) direction. The complementary analysis was performed on the ND-TD section, where TD is the transverse direction. The microscope control, the pattern acquisition and solution were carried out with the HKL Channel 5 system.

3. Results and discussion

3.1. Deformation microstructures and textures

Two sets of dislocation walls is the most preferred dislocation substructure observed in the ND-ED plane (longitudinal sections) after deformations of 40% and 60%, for both sample orientations. The differences in the inclination of the dislocation boundaries with respect to ED were due to the orientation of the initial crystal lattices. In the case of the *Goss* orientation, two symmetrically (with respect to the plane perpendicular to TD) situated pairs of co-planar slip systems operating in the planes inclined at 35° to ED ensure the stability of the sample orientation up to large strains. For the *brass* orientation, the standard crystal plasticity predicts the shears, on the same two planes, but this is as a consequence of the domination of a single slip along each plane, and therefore their strong stability in plane strain compression (PSC). The crystallographic character of the dislocation slip has been confirmed many times in the past, e.g. [10, 11] by the local orientation measurements. In both crystal orientations, the traces of the microbands boundaries correspond closely to the most privileged slip systems. Since both crystals show a relatively high orientation stability, the calculated disorientations are very low ($<10^\circ$). In the case of each sample, only small regions (close to the corners of the sample) showed a significantly stronger scattering of the orientations; the spread of the orientations was distinguished $\sim 20^\circ$. However, the disorientation axes were always lying close to TD. The stronger rotated regions were the privileged places for the nucleation of new grains after annealing.

3.2. Recrystallization behaviour

The annealing of the single crystals of the stable orientations reveals that the recrystallized grains nucleate preferentially in small areas characterized by relatively larger crystal lattice rotations (corners of the samples). The volume fraction of the recrystallized phase was small at the beginning stages of the recrystallization. In many cases, the recrystallized grains were found to have an elongated morphology with the longer axis closely parallel to the traces of the $\{111\}$ planes, on which the most active slip system operates, as visible in the EBSD maps, in Fig. 1. The orientation relationship between the deformed matrix and the recrystallized grain, usually described in the literature by $\alpha \langle 111\rangle$ or $\alpha \langle 112\rangle$ relations, is very often replaced by a rotation around other disorientation axes, e.g. $\langle 221\rangle$, $\langle 012\rangle$ or $\langle 110\rangle$, e.g. [3-8, 12].

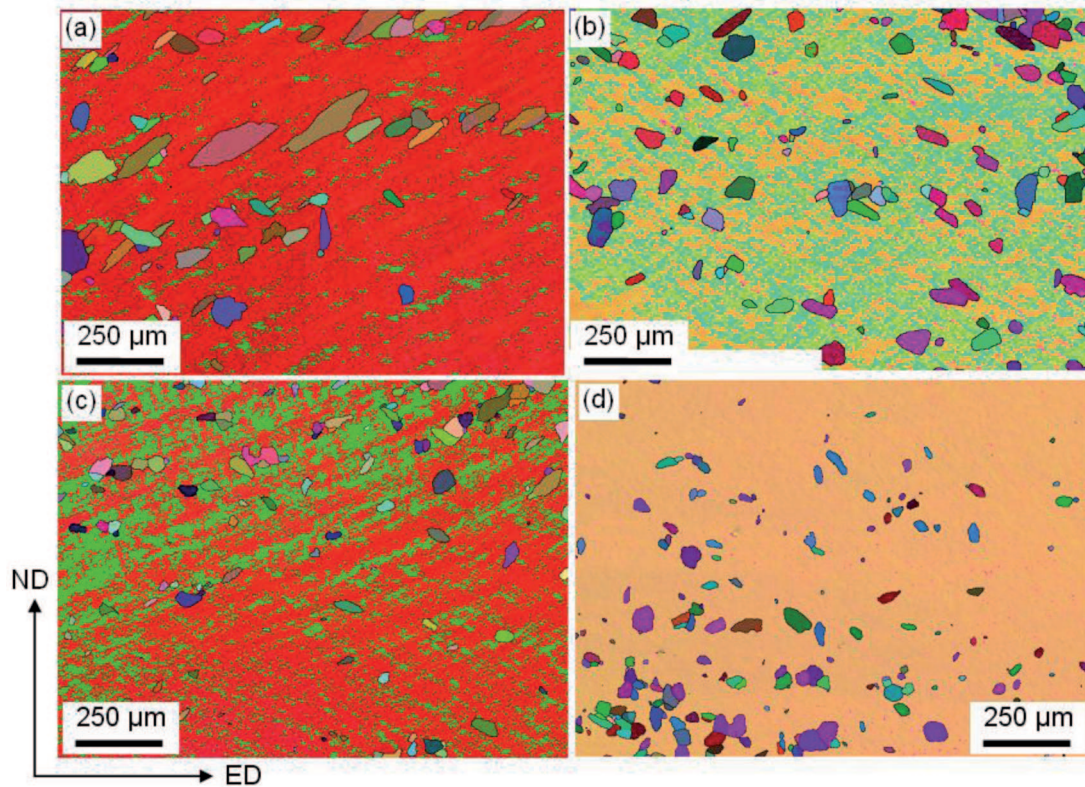


Fig. 1. EBSD maps showing the nucleation of the new grains in the samples deformed by 40%: (a) and (b) pure Al, (c) and (d) Al-1%wt.Mn alloy. (a) and (c) Goss{110}<001> and (b) and (d) brass{110}<112> orientations. Samples recrystallized for 25s at: (a) 345°C, (b) 425°C, (c) 415°C and (d) 385°C. IPF color code was applied

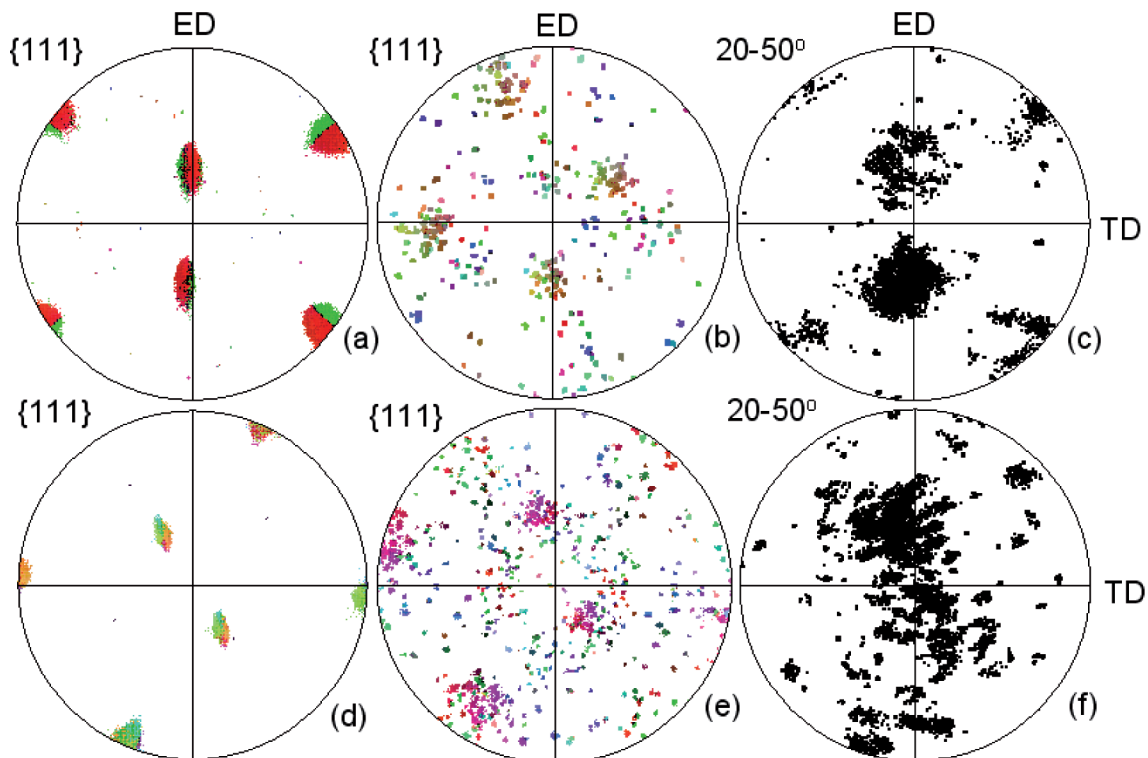


Fig. 2. Orientation relationships between the deformed areas and the recrystallized grains, corresponding structures presented in Figs. 1a and b. (a)-(c) Goss{110}<001> and (d)-(f) brass{110}<112> orientation. The {111} pole figures showing the orientation: (a) and (d) only deformed state, (b) and (e) only recrystallized grains, (c) and (f) disorientation axes distributions presented in the sample coordinate system. Pure Al deformed by 40%

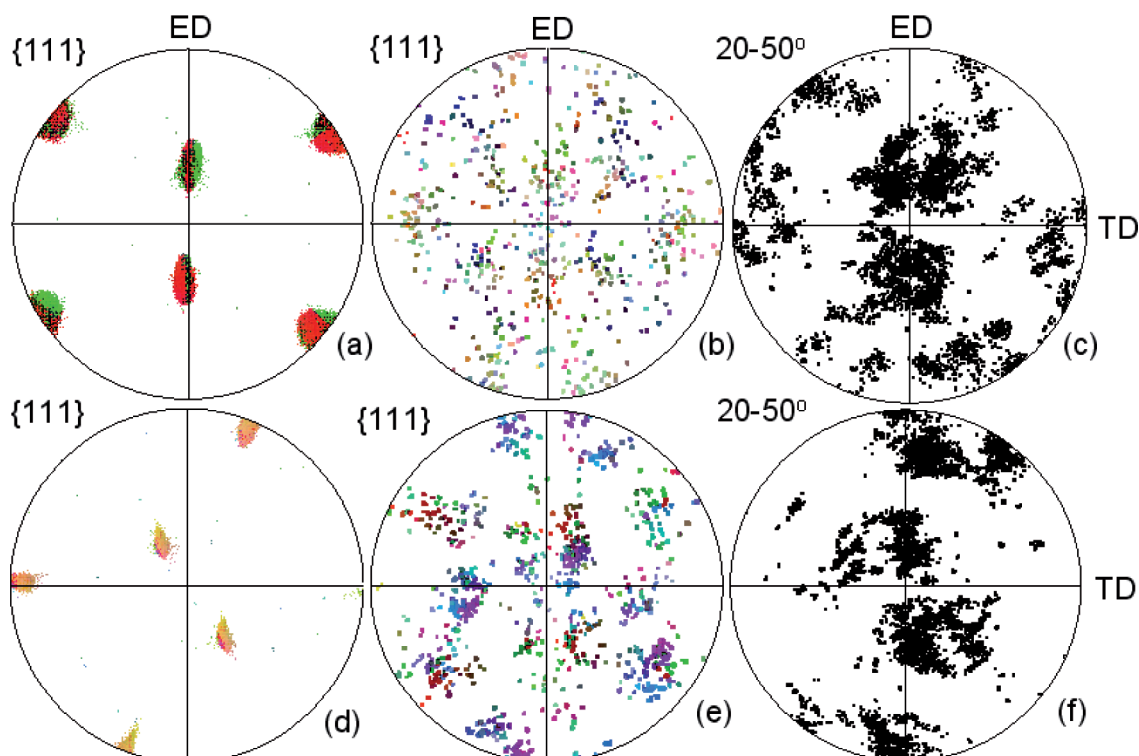


Fig. 3. Orientation relationships between the deformed areas and the recrystallized grains, corresponding structures presented in Figs. 1c and d. (a)-(c) Goss{110}<001> and (d)-(f) brass{110}<112> orientation. The {111} pole figures showing the orientation: (a) and (d) only deformed state, (b) and (e) only recrystallized grains, (c) and (f) disorientation axes distributions presented in the sample coordinate system. Al-1%wt.Mn alloy deformed by 40%

Figures 2 (for Al) and 3 (for Al-1%wt.Mn) show the {111} pole figures separately for the deformed (a) and the recrystallized (b) 'phases', as well as the corresponding distribution of the disorientation axes (in the orientation relation between the new grains and the deformed areas) presented in the sample coordinate system (c). As expected, the deformed textures show a relatively high stability for both orientations (and for both metals) after the 40% deformation (Figs. 2a, d and 3a, d). The orientations of the new isolated grains (i.e. completely surrounded by the deformed matrix) are scattered but not accidental. It is visible that some groups of orientations were more populated than the others ones. This, not accidental, 'nucleation' of the new grain orientations leads to some preferences in the distribution of the disorientation axes in the orientation relationship between the deformed and the recrystallized areas. Figures 2c, f and 3c, f show that the disorientation axes only partly coincide with the poles of the {111} planes of the deformed state. The most populated disorientation axes were slightly shifted towards the <221>, <012> or <112> positions, lying close to the selected normals of the {111} slip planes, with which the dislocation boundaries align. The most populated disorientation angle in the disorientation relation between the new grain and the deformed areas were ranged between 20° and 50°, as visible in Fig. 4.

Here, again the type of the orientation relation between the recrystallized grain and the deformed matrix is documented as not accidental. At the early stages of recrystallization, the calculated disorientations between the new grains and the deformed areas were dominated by rotations around one of the following axes: <112>, <122>, <012> or <111>. The disorientation angles were preferentially ranged between 20° and 50°. In the earlier works [3-5, 12], some of the present authors suggested that at the early stages of annealing, the observed disorientations can be 'created' by a thermally activated dislocation movement along the {111} planes, similarly to the processes observed in the deformed state. In most of the observed cases, the appearance of the specific disorientations could have been explained based on the dislocations movement (into the recrystallization front) over one or two {111}-type planes, on which the most active slip systems had dominated in the deformation process. The explanation of the <112>-type disorientation axis is relatively simple, and could be directly linked to the dislocation movement on a single {111}<011>-type system. Other cases of rotation axes which were calculated seem to be more complicated. However, in each case, the explanation of the occurrence of a specific disorientation axis can be based on the coordinated dislocation movement over two {111} planes, as presented in [4, 5, 8]. Nevertheless, the system selection of the {111} planes is still not fully clear.

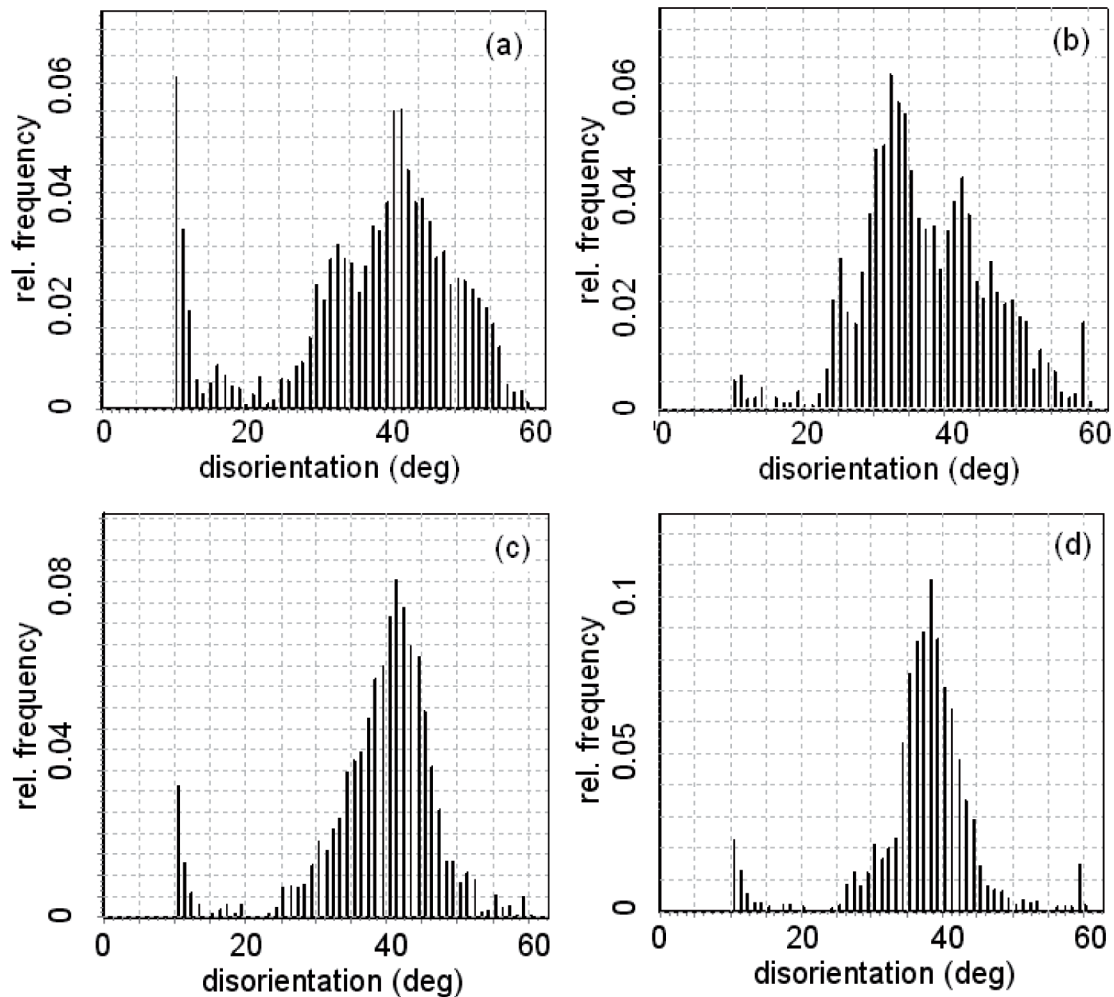


Fig. 4. Disorientation angle distributions in the relationship between the recrystallized grains and the deformed areas, corresponding structures presented in Fig. 1. (a) and (b) pure Al, (c) and (d) Al-1%wt.Mn alloy. Samples orientation: (a) and (c) Goss{110}<001>, (b) and (d) brass{110}<112>. The disorientations greater than 10° were only regarded

Okada et al [13] showed that the new grains that occurred after annealing in Al single crystals strained in tension were rotated from the initial crystal orientation around the same axis that plays the decisive role in the orientation scattering of the deformed state. In the earlier works [4, 5, 8] some of the present authors also suggested that certain rotations might have been caused by the dislocation structure introduced during the deformation. Paul and Driver [4] presented a way to create the disorientation with the rotation of about <100>, which consists in invoking a mechanism of a collective dislocation motion over the two {111} planes which were the most active in the deformed state. A similar concept based on the co-ordinated movement of the different sets of dislocation ‘families’ was also used by Bijak et al [5] for the explanation of the disorientation axes of the <012>, <122> or <011>-types, in pure Al single crystals of the unstable orientations.

Based on crystallography, the occurrence of the <111>-type disorientation axis may be explained on the

basis of the motion of two dislocation sets containing screw components (twist boundary formation) operating on the same slip plane, as presented originally by Ridha and Hutchinson [1]. A good correlation between the specific variant of the <111> rotation axes and the normal to highly active slip planes, with which the dislocation aligns, has been confirmed many times in the past, e.g. by Sabin et al. [7] or West et al [6], on cold rolled polycrystalline pure aluminium. A similar idea was used by Inoko et al [14] in their interpretation of the mechanisms of the recrystallized grain growth (after the tensile deformation) due to the boundary migration by way of absorbing the piled-up edge dislocations. The mechanism of the <111> rotation occurring in the recrystallization the authors explained by the rotation of the deformed matrix around the <111> axis normal to the common cross slip plane of the dominant slip systems of the deformed state.

The migration of the grain boundaries and the annihilation of dislocation in the deformed metals very often

occurred in the directions parallel to the traces of the {111} planes, as showed by Paul and Driver [4] in their work on the Al bicrystals. The same effect was well visible in both stable orientations, analyzed here, over a wide range of deformations. Moreover, the recrystallization front (in the direction of the privileged growth) was very irregular, independently of the as-deformed microstructure. This clearly indicates different local growth rates which are probably due to the local variations in the disorientation relation, as a consequence of the orientation spread in the deformed state.

4. Conclusions

The nucleation in a high purity Al and the Al-1%wt.Mn alloy single crystals of the stable Goss{110}<001> and brass{110}<001> orientations were investigated by SEMFEG/EBSD. The present results show that a unique preferential growth relation of the 40° <111>-type, which is very often discussed in literature, is very debatable. The disorientation angles were very often placed within a broad range, usually of 20-50°. The <111>-type disorientation is only one of the few often observed. In most cases, the orientations of the first formed nuclei were disoriented with respect to the orientations identified within the neighbouring deformed areas by rotations around the <221>, <012>, <112>, or <111> directions. The investigations of the direction of the growth indicate the privileged role of the {111} planes in the initial stages of recrystallization. In most of the observed cases, the new grains were strongly elongated with the planar facets close to those of the dislocation slip.

The migration of the newly formed grain boundaries and the 'consumption' of the deformed areas at the initial stages of recrystallization occurred by means of a mechanism that can be linked to the dislocation movement on the {111} planes. The possible orientation relations confirmed a good agreement between the rotation axes

and the highly active slip planes with which the dislocation boundaries align. The <112> rotation axes can be directly related to the strong (thermal) activity along a single {111}<011> system. To create disorientations described by other axes, one can invoke a mechanism of a collective dislocation motion over two different {111} planes of different configurations, as pointed out in the earlier works [3, 6, 8].

REFERENCES

- [1] A.A. Ridha, W.B. Hutchinson, *Acta Metall.* **30**, 1929 (1982).
- [2] R.D. Doherty, D.A. Hughes, F.J. Humphreys, J.J. Jonas, D. Juul Jensen, M.E. Kassner, et al. *Mat. Sci. Eng.* **A238**, 219 (1997).
- [3] H. Paul, J.H. Driver, C. Maurice, A. Piątkowski, *Acta Mater.* **55**, 833 (2007).
- [4] H. Paul, J.H. Driver, *Mat. Sci. Forum* **467-470**, 171 (2004).
- [5] M. Bijak, H. Paul, J.H. Driver, *J. Microscopy* **237**, 221 (2010).
- [6] S.S. West, G. Winther, D.J. Jensen, *Metall. Mater. Trans. A* **42**, 1400 (2011).
- [7] T.J. Sabin, G. Winther, D.J. Jensen, *Acta Mater.* **51**, 3999 (2003).
- [8] H. Paul, J.H. Driver, *Microchimica Acta* **155**, 235 (2006).
- [9] H. Paul, J. Driver, *Arch. Metall. Mater.* **50**, 209 (2005).
- [10] A. Godfrey, D.J. Jensen, N. Hansen, *Acta Mater.* **46**, 823 (1998).
- [11] A. Borbely, Cl. Maurice, D. Piot, J.H. Driver, *Acta Mater.* **55**, 487 (2007).
- [12] H. Paul, *Mat. Chem. Physics* **81**, 531 (2003).
- [13] T. Okada, X. Huang, K. Kashihara, F. Inoko, J.A. Wert, *Acta Mater.* **51**, 1827 (2003).
- [14] F. Inoko, K. Kashihara, M. Tagami, T. Okada, *Mater. Trans.* **51**, 597 (2010).